Lattice Boltzmann simulation of flow in porous media on non-uniform grids

H.R. Wu, Y.L. He, G.H. Tang and W.Q. Tao*
State Key Laboratory of Multiphase Flow in Power Engineering,
Xi'an Jiaotong University, Xi'an, Shaanxi 710049, P.R. China
Fax: +86 29 266 9106 E-mail: wqtao@mail.xjtu.edu.cn
*Corresponding author

Abstract: In this paper, the Lattice Boltzmann method (LBM) is adopted to simulate the incompressible flow in porous media on non-uniform grids. The flow through porous media was simulated by including the porosity into the equilibrium distribution function and adding a force term to the evolution equation to account for the linear and non-linear drag forces of the porous medium. Besides, non-uniform grids are adopted by using the interpolation-supplemented Lattice Boltzmann equation. Numerical simulations of lid-driven cavity flow, flow in a 2D symmetric sudden expansion channel, and cavity flow in polar coordinates are carried out. The results agree well with benchmark solutions, experimental data or traditional computational fluid dynamics method solutions. The present results demonstrate the potential of the Lattice Boltzmann algorithm for numerical simulation of fluid through porous media.

Keywords: Lattice Boltzmann method; flow through porous media; non-uniform grids.

Reference to this paper should be made as follows: Wu, H.R., He, Y.L., Tang, G.H. and Tao, W.Q. (2005) 'Lattice Boltzmann simulation of flow in porous media on non-uniform grids', *Progress in Computational Fluid Dynamics*, Vol. 5, Nos. 1/2, pp.97–103.

Biographical notes: H.R. Wu is a graduate student working for Master's degree of Engineering Thermophysics at the Xi'an Jiaotong University. He received his BE degree in Refrigerating and Cryogenic Engineering from Xi'an Jiaotong University in 2001. His major scientific interests are Lattice Boltzmann methods for porous media, electronics cooling techniques, and design of compact heat exchanger.

Y.L. He is a Professor of Xi'an Jiaotong University, China. She received her PhD in Engineering Thermophysics from Xi'an Jiaotong University. She has published more than 100 technical papers. She is also the author of four text and handbooks. She owns four patents in pulse tube refrigerator. Her research interests include cooling techniques of electronic devices, small-scale refrigerator and cryocooler in the high technology, computer simulation and optimisation of refrigeration system, heat exchangers with high efficiency; fluid flow and heat transfer in mirochannels, thermophysical problems in the fuel cells, new cooling technology for the rocket thruster of high pressure.

G.H. Tang is a Lecturer and PhD candidate at School of Energy and Power Engineering in the Xi'an Jiaotong University. He received his Master's degree in Thermal Engineering from the same university in 1998. His research interests include heat transfer design/management and enhancement, micro-scale heat/mass transfer, and the Lattice Boltzmann method for slip flow in porous media, multiphase flow and fluid flow and heat transfer of biofluid.

W.Q. Tao is a Professor of Engineering Thermophysics at the Xi'an Jiaotong University, China. He graduated from Xi'an Jiaotong University in 1962, and received his graduate diploma in 1966. He has written over 200 journal and has conference papers. He is also the author or coauthor of eight textbooks. He is now Member of Advisory Board of Numerical Heat Transfer, the Regional Associate Editor of *International Journal of Heat Mass Transfer*, and *Communication in Heat Mass Transfer*. His research interests include advanced computational heat transfer, heat transfer enhancement, micro- and mini-channel heat transfer, and cooling techniques of electronic devices

1 INTRODUCTION

The study of transport phenomena in porous media is a subject of wide interdisciplinary concern, with many applications in fluid mechanics, condensed matter, and life and environmental sciences as well [1]. It is also one of the important applications of the LBM. The dual field-particle character of LBM shines brightly here: the particle-like nature of LBM permits a transparent treatment of grossly irregular geometries in terms of elementary mechanics events, such as mirror and bounce-back reflections; on the other hand, the field-like nature of LBM permits achievement of fluid dynamic behaviour also in tiny interstitial regions of the flow which are hardly accessible to the macroscopic approach. These assets make LBM an excellent numerical tool for flow through porous media [2].

Two approaches have been adopted in simulations of flow in porous media by using LBM. In the first approach, the fluid in the pores of medium is directly modelled by the standard LBM [1]. The main advantage of this approach is that detailed flow information can be obtained. However, if adopting the approach, the size of computation domain cannot be too large due to limited computer resources since each pore of the medium should contain several lattice nodes. In the second approach, modelling is made for the fluid at a representative elementary volume scale. This is accomplished by including an additional term to the standard Lattice Boltzmann equation (LBE) to account for the presence of a porous medium [3]. In this approach, the detailed structure is ignored, and the statistical properties of the medium are directly included in models. Although detailed information of fluid flow at the pore scale is unavailable, if this approach can be used in large-sized computation domain and with appropriate models, the approach can produce reasonable results. In the simulation of fluid flow and heat transfer in the shell-side of a shell-and-tube heat exchanger, such approach is the only applicable one by the numerical method based on the continuum assumption [4–6], at least at the present development stage of computer technology.

The grid in previous LB models has usually been limited to a rectangular and uniform grid system. It is obvious that the Lattice Boltzmann methods can be made more computationally useful by generalising them to apply to non-rectangular and non-uniform grids. With an efficient treatment of a non-rectangular and non-uniform mesh, curved boundary can be described more accurately and computational resource can be used more efficiently. In an effort to implement the LB method on a non-uniform mesh, an interpolation-supplemented Lattice Boltzmann equation (ISLBE) model was proposed in [7,8]. The basic idea of ISLBE was based on the fact that the density distribution is a continuous function in physical space and can be well defined for any mesh system. Density distribution functions at non-grid points can always be calculated by interpolation from those of their surrounding grid nodes.

In the present work, we adopt the Lattice Boltzmann model for porous medium of the second approach [3] and apply it to non-uniform grids generated using the technique developed in [7,8]. Numerical simulations of the lid-driven cavity flow, the flow in a 2D symmetric sudden expansion channel, and the cavity flow in polar coordinates are carried out. It is found that the results agree well with benchmark solutions, experimental data or the solutions of traditional computational fluid dynamics method.

2 LATTICE BOLTZMANN MODEL FOR POROUS MEDIA

For the numerical approach based on the continuum assumption, Nithiarasu and Ravindran [9] adopted a model which is applicable for a medium with both a constant and a variable porosity under the consideration of porosity effect. The model can be expressed by the following equations.

$$\nabla \cdot \boldsymbol{u} = 0 \tag{1a}$$

$$\frac{\partial \boldsymbol{u}}{\partial t} + (\boldsymbol{u} \cdot \nabla)\left(\frac{\boldsymbol{u}}{\varepsilon}\right) = -\frac{1}{\rho}\nabla(\varepsilon p) + \upsilon_e \nabla^2 \boldsymbol{u} + \boldsymbol{F} \tag{1b}$$

where ρ is the fluid density $\boldsymbol{u}$, p and ε the volume-averaged velocity, pressure and porosity, respectively, and υ_e the kinetic viscosity of fluid. $\boldsymbol{F}$ represents the total body force due to the presence of a porous media and other external force fields, and is given by [9]

$$\boldsymbol{F} = -\frac{\varepsilon \upsilon}{K}\boldsymbol{u} - \frac{\varepsilon F_\varepsilon}{\sqrt{K}}|\boldsymbol{u}|\boldsymbol{u} + \varepsilon \boldsymbol{G} \tag{2}$$

where

$$F_\varepsilon = \frac{1.75}{\sqrt{150\varepsilon^3}} \tag{3a}$$

$$K = \frac{\varepsilon^3 d_p^2}{150(1-\varepsilon)^2} \tag{3b}$$

where d_p is the solid particle diameter and **G** is the gravitational acceleration.

Guo and Zhao [3] introduce this idea to the LBM. To include the effect of the porous media, they define the equilibrium distribution function as

$$f_i^{\mathrm{eq}} = \omega_i \rho \left[1 + \frac{(\boldsymbol{c}_i \cdot \boldsymbol{u})}{c_s^2} + \frac{(\boldsymbol{u} \cdot \boldsymbol{c}_i)^2 - (c_s^2 \boldsymbol{u}^2)}{2\varepsilon c_s^4}\right] \tag{4}$$

where ω_i is the weight and c_s is the sound speed. Both ω_i and c_s depend on the underlying lattice. The weights are given by $\omega_0 = 4/9$, $\omega_i = 1/9$ for $i = 1$–4, $\omega_i = 1/36$ for $i = 5$–8, and $c_s = C/\sqrt{3}$, where $c = \Delta x/\Delta t$ and Δx is the lattice spacing.

For the D2Q9 model, the velocity vectors $\mathbf{c}_i$ are defined as [10]

$$\boldsymbol{c}_i = \begin{cases} 0 & i=0 \\ \left(cos\left[(i-1)\frac{\pi}{2}\right], sin\left[(i-1)\frac{\pi}{2}\right]\right)\cdot C & i=1,2,3,4 \\ \sqrt{2}\left(cos\left[(i-5)\frac{\pi}{2}+\frac{\pi}{4}\right], \right. & \\ \left. sin\left[(i-5)\frac{\pi}{2}+\frac{\pi}{4}\right]\right)\cdot C & i=5,6,7,8 \end{cases} \tag{5}$$

Adding a force term into the Lattice Boltzmann equation to account for the force due to the presence of a porous media, the discretised equation can be written as [3]

$$f_i(\boldsymbol{x}+\boldsymbol{c}_i.\Delta t, t+\Delta t) - f_i(\boldsymbol{x},t) = \frac{1}{\tau}[f_i^{eq}(\boldsymbol{x},t) - f_i(\boldsymbol{x},t)] + \Delta t F_i \tag{6}$$

where

$$F_i = \omega_i \rho\left(1-\frac{1}{2\tau}\right)\left[\frac{\boldsymbol{c}_i\cdot\boldsymbol{F}}{c_s^2} + \frac{(\vec{\boldsymbol{u}}\cdot\boldsymbol{c}_i)(\boldsymbol{F}\cdot\boldsymbol{c}_i) - \vec{u}\cdot\boldsymbol{F}}{\varepsilon c_s^4}\right] \tag{7}$$

The density ρ, and velocity $\mathbf{u}$ are obtained from [3]

$$\rho = \sum_i f_i \tag{8}$$

$$\rho\boldsymbol{u} = \sum_i \boldsymbol{c}_i f_i + \frac{\delta_t}{2}\rho\boldsymbol{F}. \tag{9}$$

3 LATTICE BOLTZMANN MODEL FOR NON-UNIFORM GRID SYSTEM

On a rectangular uniform grid system, starting from one grid site x, the distribution function f_i advected to a neighbouring grid site during each time step. Since the lattice separation Δ_x equals $c\Delta_t$, the distribution function at all grid nodes is exactly known at the next time step, and the evolution continues. On an irregular grid, however, the end point of the streaming process is generally no longer a grid node of the irregular non-uniform grid system. The determination of the poststreaming distribution function at grid nodes of the non-rectangular and non-uniform grid system is essential for the implementation of the LB method on an irregular grid.

In the interpolation-supplemented Lattice Boltzmann method, the unknown poststreaming distribution functions at the irregular grid nodes can be calculated by interpolation using their neighbouring shifted grid nodes. In this paper, we choose to formulate the interpolation procedure in a curvilinear coordinate system. The flow domain can be described by a curvilinear coordinate system, $\xi = \xi(\boldsymbol{x})$ and $\eta = \eta(\boldsymbol{x})$, where $\boldsymbol{x}$ is a cartesian coordinate system. The computational domain in the curvilinear coordinate system can be projected onto a uniform grid. The relative position of an original grid node $\boldsymbol{x}$ to its shifted correspondent (ξ_i,η_i), can be written as [7]

$$d\xi_i = \xi(x - c_i\Delta_t) - \xi_i \tag{10a}$$

$$d\eta_j = \eta(x - c_i\Delta_t) - \eta_j \tag{10b}$$

The poststreaming distribution at the original grid node can be calculated using a second-order upwind interpolation [7].

$$f_i(\mathbf{x}, t+1) = \sum_{k=0}^{2}\sum_{l=0}^{2} a_{m,k} b_{n,l} f_i(\xi^x_{m+k\times md}, \eta^y_{n+l\times nd}, t+\Delta 1) \tag{11}$$

where $md = sign(1,d\xi)$ and $md = sign(1,d\eta)$ which determine the interpolation direction. The interpolation coefficients are calculated by [7]

$$a_{m,0} = \frac{(|d\xi_i| - \Delta\xi)(|d\xi_i| - 2\Delta\xi)}{2\times\Delta\xi^2} \quad b_{n,0} = \frac{(|d\eta_j| - \Delta\eta)(|d\eta_j| - 2\Delta\eta)}{2\times\Delta\eta^2}$$
$$a_{m,1} = -\frac{|d\xi_i|(|d\xi_i| - 2\Delta\xi)}{\Delta—^2} \quad b_{n,1} = -\frac{|d\eta_j|(|d\eta_j| - 2\Delta\eta)}{\Delta\eta^2}$$
$$a_{m,2} = \frac{|d\xi_i|(|d\xi_i| - \Delta\xi)}{2\times\Delta\xi^2} \quad b_{n,2} = \frac{|d\eta_j|(|d\eta_j| - \Delta\eta)}{2\times\Delta\eta^2} \tag{12}$$

where $\Delta\xi$ and $\Delta\eta$ are the grid spacings in the curvilinear coordinate system.

4 NUMERICAL SIMULATION RESULTS AND DISCUSSION

To validate the present model, we applied it to three typical 2D problems: lid-driven cavity flow, flow in a 2D symmetric sudden expansion channel and cavity flow in polar coordinates. We adopt non-uniform grids which are finer in the complex flow region. Obviously, as ε approaches 1, the porous media effect can be ignored and the flow resumes to the conventional one. Therefore, we firstly set $\varepsilon = 0.99$ and compare the results with benchmark solutions. Then, flows in porous medium are simulated and the results are compared with solutions for porous medium obtained from the finite volume method.

4.1 Lid-driven flow

Due to the simple geometry and complicated flow behaviours, lid-driven cavity flow has been used as a benchmark problem. We simulate the flow in a square cavity whose height and width are the same and is filled with porous media. The left, right and bottom walls of the cavity are fixed, and the upper wall moves from left to right with a constant velocity u_0. Flow field is initialised by setting $\rho = 2.7$ and $u = 0$. At left, right and bottom walls, bounce-back boundary conditions are applied. At upper wall, mirror-reflecting boundary condition is applied. The grid is finer near the top because the flow in the near top-wall region is much stronger than elsewhere. The computational grid for the square cavity is shown in Figure 1.

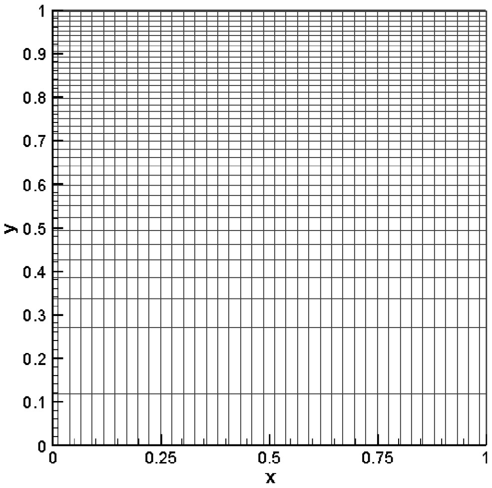

Figure 1 *Mesh grids for square cavity*

In Figures 2 and 3, we compare the LB solutions for $\varepsilon = 0.99$, $\mathrm{Da} = K/L^2 = 10^4$, and $\mathrm{Re} = 1000$ with benchmark solution for the conventional fluid in [11]. A good agreement can be clearly observed. For comparison, the flow is also solved by finite volume method (FVM). In Figures 4 and 5, we compare the LB solutions for porous medium with FVM solutions. From the figures, it can be seen that the agreements between the LB simulation and benchmark solutions or FVM solutions are fairly good. In Figure 6, the effect of Da on the flow pattern is presented. As seen there, with the decrease in Da number, lid-driven effect becomes stronger and the boundary layer becomes thinner.

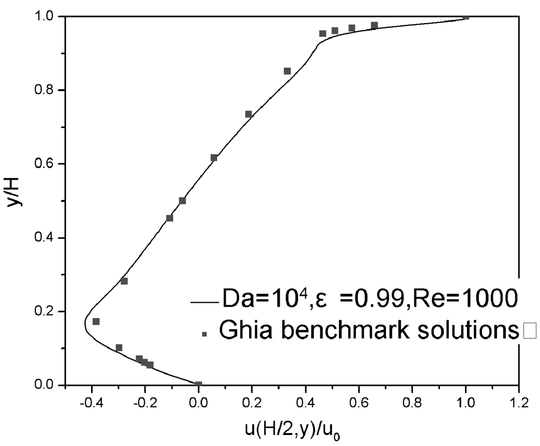

Figure 2 *Velocity profiles of the cavity centre u component normalised by u_0 at $X = x/L = 0.5$*

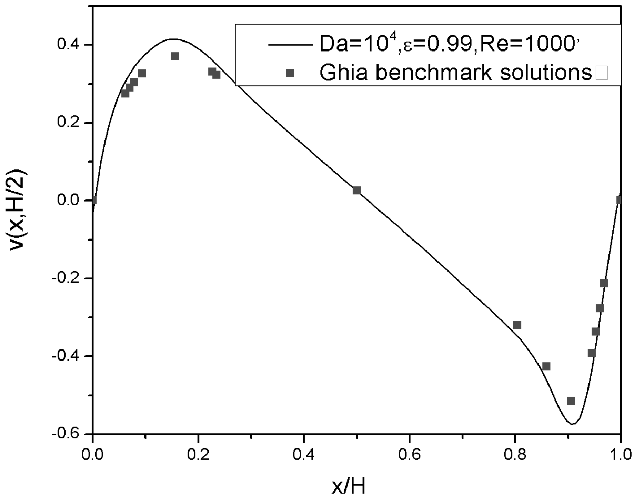

Figure 3 *Velocity profiles of the cavity centre v component normalised by u_0 at $Y = y/L = 0.5$*

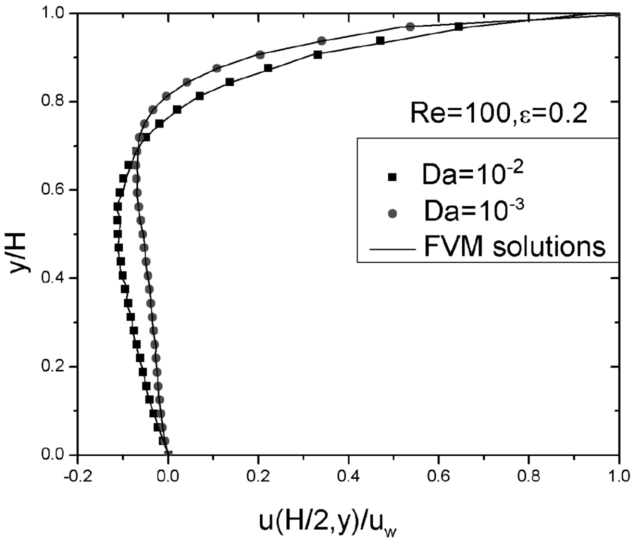

Figure 4 *Velocity profiles of the cavity centre u component normalised by u_0 at $X = 0.5$*

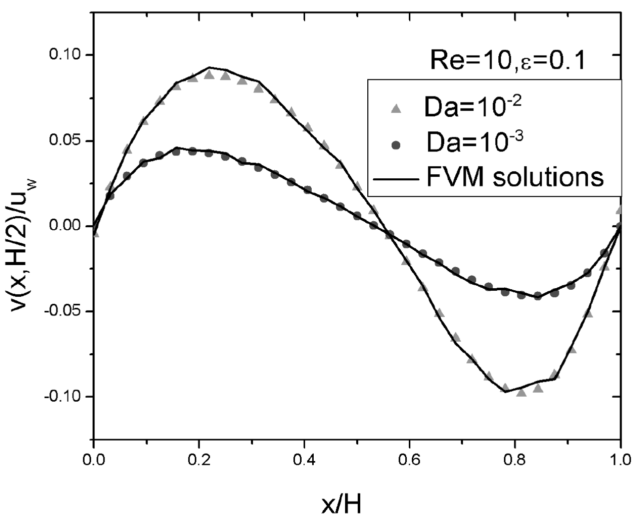

Figure 5 *Velocity profiles of the cavity centre v component normalised by u_0 at $Y = 0.5$*

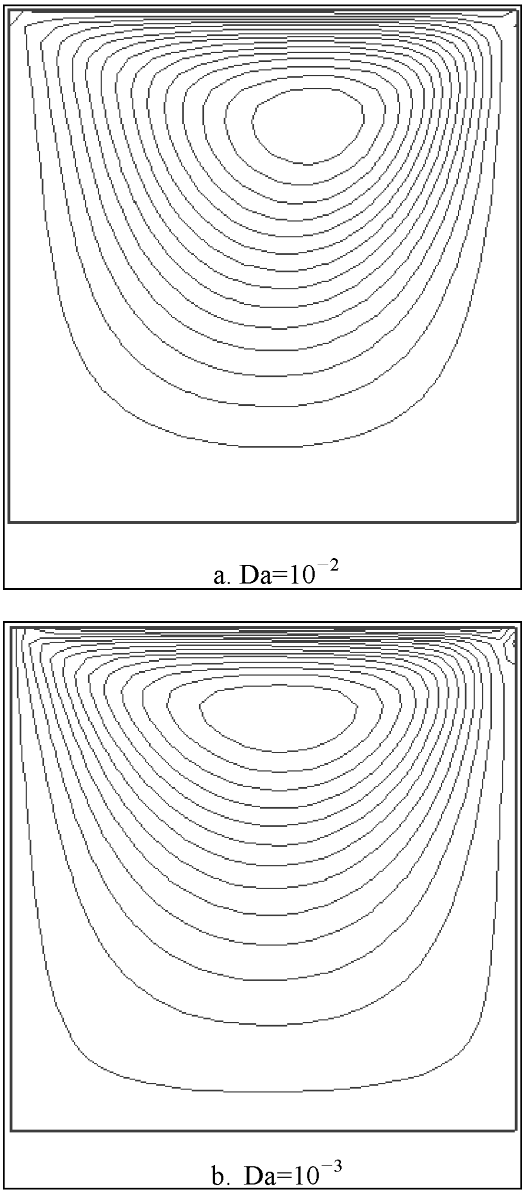

Figure 6 *Streamlines for ε = 0.99 a. Da = 10^{-2} b. Da = 10^{-3}*

4.2 Flow in a 2D symmetric sudden expansion channel

The flow in a symmetric channel with sudden expansion is a hydrodynamic system with an array of interesting phenomena, including symmetry breaking bifurcations and a specific route to turbulence. Although the system possesses complicated hydrodynamic phenomena, the geometry of this system is very simple. It is relatively easy to generate a non-uniform mesh. A 2D channel with an expansion ratio of 1:8 filled with porous media is studied. At entrance, a parabolic profile of the horizontal component of velocity with the maximum velocity u_w is enforced, and the vertical component, u_y, is set to zero. At the exit, a fully developed condition is enforced. At the walls, a bounce-back boundary condition is applied. Flow field is initialised by setting $\rho = 2.7$ and $u = 0$. The grid is finer near inlet because the flow in the domain is unstable. The computational grid for the sudden expansion channel is shown in Figure 8.

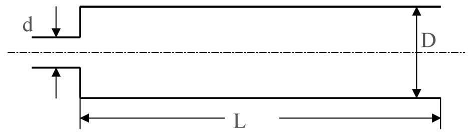

Figure 7 *Sudden expansion channel*

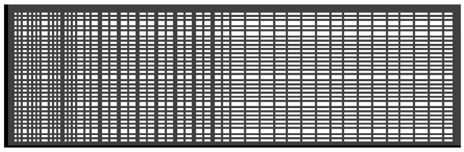

Figure 8 *Mesh grids for sudden expansion tube channel*

In Figure 9, we compare the solutions for $\varepsilon = 0.99$, Re = 10 to 400 with the experimental data in [12]. For comparison, the flow is also solved by FVM. In Figure 10, we compare the LB solutions with FVM solutions. From the figures, the good agreements between the LB simulation and results or FVM solutions are clearly shown. It is also shown that as Re increases, the asymmetry trend of velocity field becomes stronger.

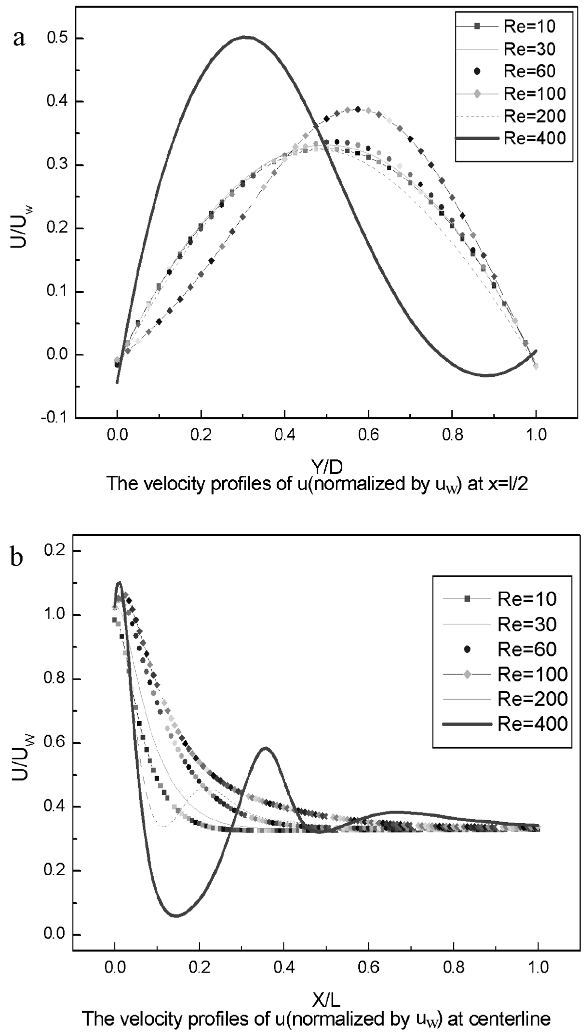

Figure 9 *Velocity profiles for ε = 0.99 through channel centre. Solid lines are LB solutions, and symbols are experimental data in [12]*

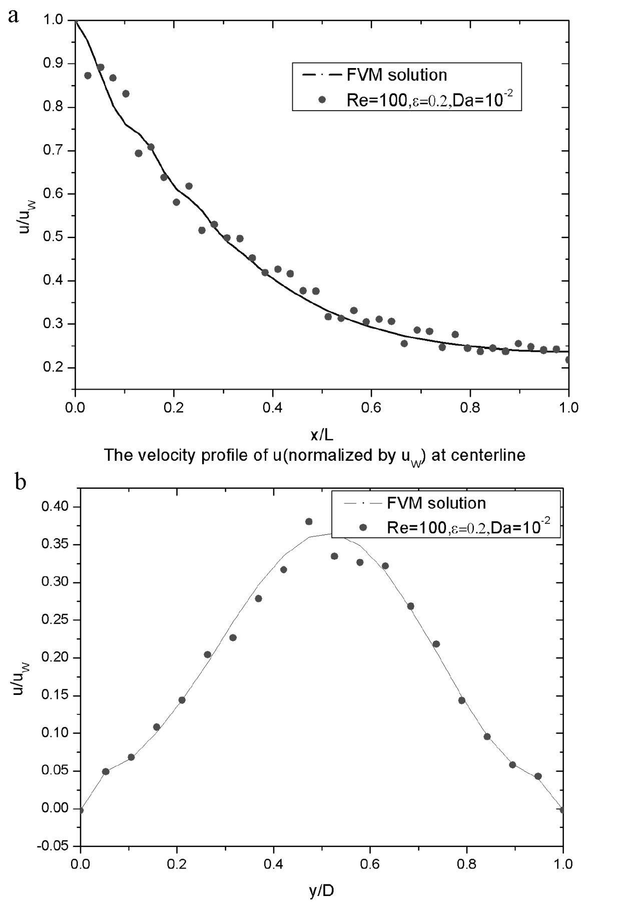

Figure 10 *Velocity profile through channel centre. Symbols represent LB solutions*

4.3 Cavity flow in polar coordinates

Curvilinear coordinates are often used in numerical simulations. In this paper, we choose cavity flow in polar coordinate to practice the interpolation method in curvilinear coordinate. A sector cavity filled with porous media is studied. The left, right and bottom walls of the cavity are fixed, and the upper wall moves from left to right with a constant velocity u_0. Flow field is initialised by setting $\rho = 2.7$ and $u = 0$. At left, right and bottom walls, bounce-back boundary conditions are applied. At upper wall, mirror-reflecting boundary condition is applied. Grids in computational domain and physical domain are shown in Figure 11.

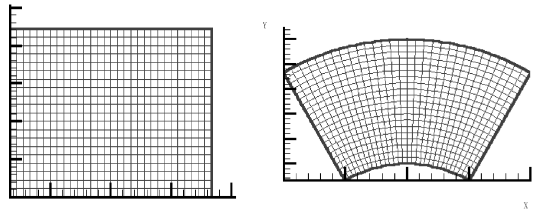

Figure 11 *Grids in computational domain and physical domain*

In Figure 12, we show the streamlines for $\varepsilon = 0.99$, Re changing from 100 to 2000. The results agree well with the finite difference solutions in [13]. It is also shown that as Re increases, the vortex in the cavity becomes stronger.

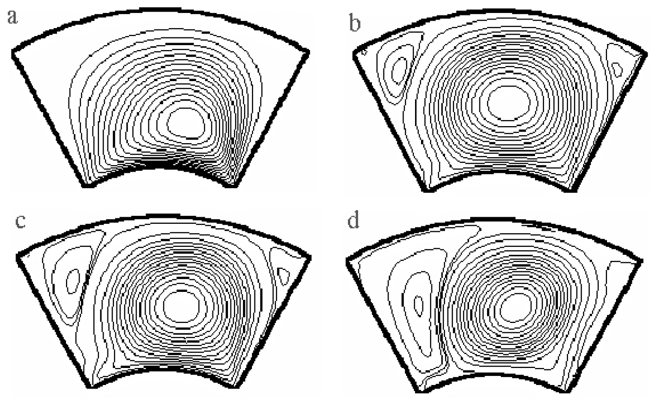

Figure 12 *Streamlines for $\varepsilon = 0.99$ (a) Re = 100 (b) Re = 400 (c) Re = 1000 (d) Re = 2000*

5 CONCLUSIONS

In this paper, a Lattice Boltzmann algorithm is proposed to simulate flow through porous media. We take porous media effect into consideration by including the porosity into the equilibrium distribution and adding a force term to the evolution equation. Besides, we use non-uniform grids in this algorithm by adding an interpolation step between the streaming and relaxation steps. The results agree well with benchmark solutions, experimental data or the traditional computational fluid dynamics method solutions. This algorithm does not change the locality of the LB method. Because the interpolation coefficients are flow field independent and can be calculated initially, the interpolation step does not increase the computation significantly. The new algorithm retains the advantages of the Lattice Boltzmann method: parallel of algorithm, ease of programming. In the present work, we only apply the algorithm in invariable porosity without a phase change. Variable porosity and multiphase flow study will be done in the future.

ACKNOWLEDGEMENTS

This work was supported by the National Fundamental R&D Project of China (No. G2000026303) and the National Natural Science Foundation of China (No. 50236010).

REFERENCES

1 Succi, C. (2001) *Lattice Boltzmann Equation for Fluid Dynamics and Beyond*, Clarendon Press, Oxford.

2 Tao, W.Q. (2000) *Recent Advances in Computational Heat Transfer*, Science Press, Beijing.

3 Guo, Z.L. and Zhao, T.S. (2002) 'Lattice Boltzmann model for incompressible flows through porous media', *Physical Review E,* Vol. 66, No. 036304.

4 Patankar, S.V. and Spalding, D.B. (1974) 'A calculation procedure for the transient and steady state behavior of shell-and-tube heat exchanger', in Afgan, N.F. and Schlunder, E.U. (Eds.): *Heat Exchanger: Design and Theory Source Book*, McGraw-Hill, New York, pp.155–176.

5 Prithiviraj, M. and Andrew, M.J. (1998) 'Three dimensional numerical simulation of shell-and tube heat exchanger, Part 1: foundation and fluid mechanics', *Numerical Heat Transfer*, Part A, Vol. 33, pp.799–816.

6 Prithiviraj, M. and Andrew, M.J. (1998) 'Three dimensional numerical simulation of shell-and tube heat exchanger, Part 2: heat transfer', *Numerical Heat Transfer*, Part A, Vol. 33, pp.817–828.

7 He, X.Y., Luo, L.S. and Micah, D. (1996) 'Some progress in Lattice Boltzmann method, Part I: nonuniform mesh grids', *Journal of Computational Physics*, Vol. 129, pp.357–363.

8 He, X.Y. and Doolen, G. (1997) 'Lattice Boltzmann method on curvilinear coordinates system: flow around a circular cylinder', *J. Comput. Phys.*, Vol. 134, pp.306–315.

9 Nithiarasu, P. and Ravindran, K. (1998) 'A new semi-implicit time stepping procedure for buoyancy driven flow in a fluid saturated porous medium', *Comput. Methods Appl. Methods Appl. Mech. Eng*., Vol. 165, pp.147–154.

10 Hou, S.L., Zou, O.S. and Chen, S.Y. *et al*. (1995) 'Simulation of flow by the Lattice-Boltzmann method', *J. Comput. Phys.*, Vol. 118, pp.329–347.

11 Ghia, U., Ghia, N. and Shin, C.Y. (1982) 'High-Re solution for incompressible flow using the Navier-Stokes equations and a multigrid method', *J. Comput. Phys*., Vol. 48, pp.387–411.

12 Fearn, R.M., Mullin, T. and Cliffe, K.A. (1990) 'Nonlinear flow phenomena in symmetric sudden expansion', *J. Fluid Mech*., Vol. 211, pp.595–608.

13 Fuchs, L. and Tillmark, N. (1985) 'Numerical and experimental study of driven flow in a polar cavity', *Int. J. Num. Meth. Fluids*., Vol. 5, pp.311–329.